Improved adsorption of streptomycin onto *Thalia dealbata* activated carbon modified by sodium thiosulfate

Lihui Huang*, Gang Li, Bing Wang, Ji Huang, Bo Zhang

Shandong Provincial Key Laboratory of Water Pollution Control and Resource Reuse, School of Environmental Science and Engineering, Shandong University, Jinan 250100, China
Tel. +86 531 88366873; Fax: +86 531 88364513; email: huanglihui9986@126.com

ABSTRACT

Sodium thiosulfate–modified activated carbon (TDAC-ST) was prepared from *Thalia dealbata*, and its ability to remove streptomycin (STM) from aqueous solutions was examined. The surface properties of TDAC-ST and the original carbon (TDAC) were also measured by scanning electron microscopy, N_2 adsorption/desorption isotherms, Fourier transform infrared spectroscopy, and energy dispersive spectroscopy. The results indicated that modification with sodium thiosulfate slightly decreased the carbon's surface area but introduced more functional groups and improved the adsorption ability greatly as compared to the original carbon. The effects of solution pH, initial STM concentration and contact time on adsorption system were also studied. The kinetics data followed the pseudo-second-order kinetics model, and the adsorption isotherms fit the Langmuir isotherm equation quite well, and the maximum adsorption capacity of was 247.65 and 170.84 mg/g for TDAC-ST and TDAC, respectively. The results indicated that sodium thiosulfate modification could greatly enhance the adsorption of STM onto activated carbon, and TDAC-ST was a promising adsorbent for the removal of streptomycin from aqueous solutions.

Keywords: Activated carbon; Sodium thiosulfate modified; Streptomycin; *Thalia dealbata*
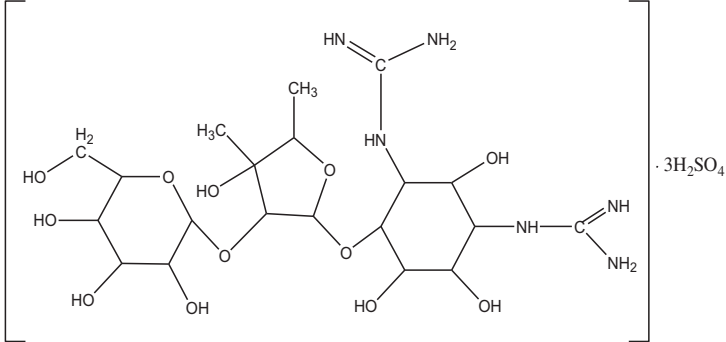
1. Introduction

Due to extensive use of antibiotics in medicine, animal husbandry and agriculture, antibiotic resistance has become a global problem that threatens the health of humans and animals as well as the function of ecosystem [1–3]. But antibiotics in wastewater are difficult to be degraded because of their high COD values and inhibition to micro-organisms [4,5]. Streptomycin (STM) is a type of the glucosamine antibiotics which is widely used to cure tuberculosis [6,7]. It is easy for bacteria to acquire resistance after contacting with STM [8] and improper use of STM would result in damage of the auditory nerve and kidney [9]. However, attention that has been paid to STM is far from enough.

Compared with treatment technologies that are used for the removal of antibiotics, such as physical/chemical treatment, biotreatment and combined biochemical treatment, adsorption has been proved to be an effective and economical method [10–12]. To our knowledge, STM from wastewater is commonly disposed by biotreatment technology and limited study has been carried out on STM removal by

*Corresponding author.

Table 1
Molecular structure of STM sulfate

Name	Molecular structure
Streptomycin sulfate (STM)	

adsorption method using activated carbons. Activated carbon is widely used in removing organic pollutants and heavy metals owing to its exceptionally high surface areas, well-developed porosity and excellent adsorption capacity [13–15]. Moreover, it is generally accepted that activated carbon modified by appropriate chemicals could greatly improve its adsorption capacity to certain hazardous substances [16]. A large amount of researches on modification of activated carbon has been emerged [17–19]. Sodium thiosulfate is commonly used as antidote in medical for its strong complexion ability and reducibility [20]. In previous study, it has been used to deal with the side effect of amino-glycoside antibiotics [21]. Therefore, sodium thiosulfate was chosen to modify activated carbon in our study, aiming to enhance its adsorption capacity of STM.

Thalia dealbata is a kind of perennial emergent macrophyte that was introduced into China recently and now frequently planted in the lakes or wetlands. It has excellent ornamental value and can purify waste water as well as absorb nitrogen and phosphorus from eutrophic water [22]. However, due to its strong occupation, rapid propagation and difficult eradication, *T. dealbata* may have great potential invasion risk and therefore may pose a serious threat to the structure and function of ecosystem. Using *T. dealbata* as precursor to prepare activated carbon can take full advantage of abundant *T. dealbata* and relieve its damage to the ecosystem. To our knowledge, no researches of adsorption on *T. dealbata* activated carbon have emerged.

In this research, activated carbon was prepared from *T. dealbata* using H_3PO_4 as chemical agent (TDAC), the prepared carbon was modified with sodium thiosulfate and removal of STM from aqueous solution was investigated. Adsorption experiments under various conditions including solution pH, initial STM concentration and contact time were performed. Additionally, adsorption kinetics, isotherms as well as thermodynamics of TDAC and TDAC-ST were conducted to understand the mechanism, confirming the feasibility of activated carbon modified by sodium thiosulfate to enhance the adsorption performance.

2. Materials and methods

2.1. Materials

T. dealbata used in this study was obtained from Daming Lake, Shandong Province. STM sulfate (USP grade) was purchased from Shanghai. Molecular structure was shown in Table 1. All chemicals used were analytical grade, and distilled water was used as experimental water.

2.2. Preparation and modification of activated carbon

T. dealbata (TD) was rinsed firstly and dried in the sunlight after received from artificial wetlands. The dried materials were then crushed and sieved into small pieces (0–1 mm) with a grinder. Afterwards, the precursor was impregnated in phosphoric acid (40 wt.%) thoroughly at a ratio of 1:2 (g TD/g H_3PO_4) and the sample underwent ultrasonic treatment for 20 min to achieve homogeneous mixing. Then, the precursor was carbonized at 500°C for 1 h in a muffle furnace. After cooling down to room temperature, the product was washed with distilled water until pH of the filtrate was steady. The sample was filtrated and dried at 120°C for 3 h. The dried sample was sieved to 100 mesh by standard sieves (Model Φ200) and stored

in a desiccator for further experimental use. The product was referred to as TDAC.

Modification of activated carbon was performed as follows: 1.0 g of TDAC was added to 100 mL of sodium thiosulfate solution at a concentration of 2–100 g/L and shaken in an oscillator at 30°C for 24 h, followed by filtration from the solvent with a vacuum pump and washed with sufficient water. Then, the obtained mass was further dried at 100°C for 12 h and also stored in desiccators. Sodium thiosulfate–modified TDAC was named as TDAC-ST-initial sodium thiosulfate concentration. For instance, TDAC-ST-2 is TDAC modified by 2 g/L of sodium thiosulfate.

2.3. Characterization methods

The BET surface areas and pore size distribution of TDAC and TDAC-ST were measured by N_2 adsorption/desorption isotherms at 77 K using a surface area analyzer (Quantachrome Corporation, USA). Manufacture's software was employed to calculate the specific surface area (S_{BET}) and the total pore volume (V_{tot}). The external surface area (S_{ext}), micropore surface area (S_{mic}), and micropore volume (V_{mic}) were obtained using t-plot method. The mean pore diameter, D_P, was calculated by $D_P = 4\ V_{tot}/S_{BET}$. The pore distribution was determined by the density unctional theory method. Surface morphology of TDAC and TDAC-ST was characterized by scanning electron microscope (SEM) analysis (JEOL JSM-7600F SEM, Japan). Functional groups were detected in the range 400–4,000 cm^{-1} using a Fourier transform infrared spectrometer (FTIR) (Fourier-380 FTIR, USA). The element analysis of TDAC and TDAC-ST was obtained from a CHN-O-Rapid Elemental Analytical Instrument (Elementer, Germany).

2.4. Adsorption experiments

2.4.1. STM adsorption studies

Batch equilibrium STM adsorption studies were performed by mixing 0.1 g of adsorbents with 100 mL solutions of varied initial concentrations (25–400 mg/L) in a series of 250-mL Erlenmeyer flasks, and the flasks were shaken at 300 rpm in a water bath shaker (SHZ-88) at 303 K until equilibrium. Then, the mixture was filtered, and the residual STM concentrations were measured according to the method [23] using an UV–vis spectrophotometer (UV-754, Shanghai, China) at a wavelength of 323 nm. In pH study, the initial solution pH was adjusted to 2–11 with 0.1 M HCl or 0.1 M NaOH solutions and pH were measured by a pH

meter (Model pHS-3C, Shanghai, China). Adsorption isotherm experiments were performed at 303, 313 and 323 K. The uptake amount Q_e (mg/g) and removal efficiency of STM at equilibrium can be calculated as follows:

$$Q_e = \frac{(C_0 - C_e)V}{W} \tag{1}$$

$$\%\ \text{Removal} = \frac{100\ (C_0 - C_e)}{C_0} \tag{2}$$

where C_0 (mg/L) and C_e (mg/L) are the initial and equilibrium concentrations of STM solutions, respectively. V (L) is the volume of the solution and W (g) is the mass of TDAC or TDAC-ST.

2.4.2. Adsorption kinetics

Adsorption kinetic experiments were performed in order to study the effect of contact time and evaluate the kinetic properties. TDAC/TDAC-ST (1.0 g) was added into 1,000 mL of STM solution with initial concentrations of 400 mg/L. The solution pH was natural detecting with a pH meter. Then, the mixture was agitated on a magnetic stirrer (HJ-3, Jintian Medical Instrument Corporation) at a speed of 300 rpm with a temperature control of 303 K. At preset time intervals, 10 mL samples were taken to filter using 0.45 μm millipore membrane filters for analysis using the same method described above.

The adsorption amount at time t (min), Q_t (mg/g), was calculated by the following equation:

$$Q_t = \frac{(C_0 - C_t)V}{W} \tag{3}$$

where C_0 and C_t (mg/L) represent the concentrations of TC solutions at initial and time t, respectively.

3. Results and discussion

3.1. Characteristics of TDAC and TDAC-ST

3.1.1. Textural characteristics of TDAC and TDAC-ST

SEM technique was widely used to study the surface morphological features of the adsorbent materials. The SEM profiles of TDAC and TDAC-ST are presented in Fig. 1. Both the samples are all porous and have rough surfaces and irregular porous structure, which are beneficial to adsorption. No big
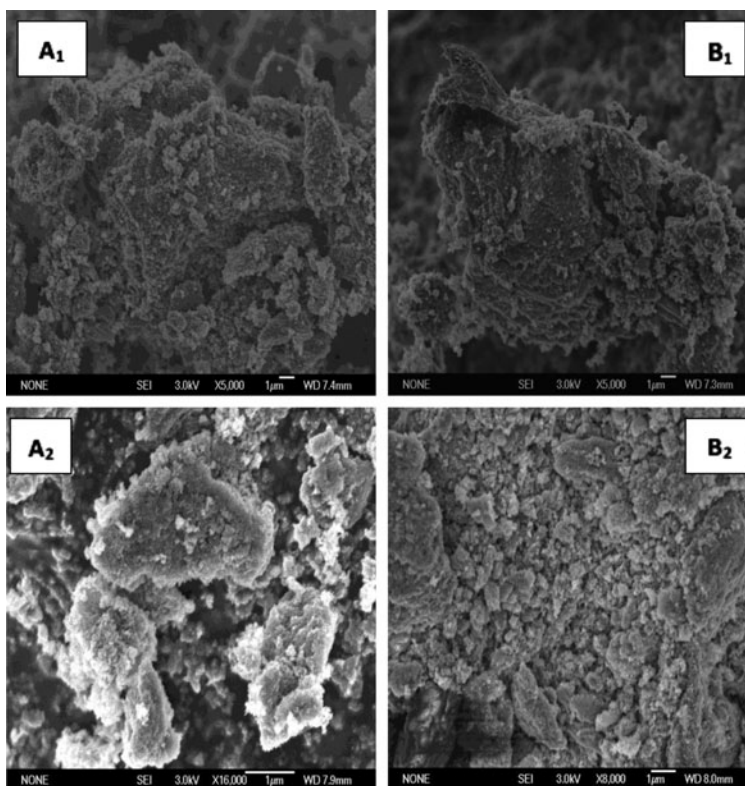
Fig. 1. SEM micrograph of TDAC (A_1 and A_2) and TDAC-ST (B_1 and B_2).

Table 2
Surface area and element analysis TDAC and TDAC-ST

	TDAC	TDAC-ST-2	TDAC-ST-10	TDAC-ST-50	TDAC-ST-100		
Surface (m^2/g)	949.28	941.78	956.46	744	557.8		
Element analysis (wt.%)	C	O	Mg	P	Ca	Na	S
TDAC	71.59	24.15	0.31	3.51	0.34		
TDAC-ST	82.06	16.00		0.69		1.00	0.25

difference in appearance was observed between the two adsorbents which indicated that the modification process did not change the external morphology of activated carbon.

Specific surface area is another significant indicator for adsorbent materials. Based on the N_2 adsorption/desorption isotherms at 77 K, the surface areas (S_{BET}) of TDAC and modified TDAC with different sodium thiosulfate concentrations are shown in Table 2. The calculated BET surface area of TDAC is 949.28 m^2/g and the concentration of sodium thiosulfate has a great impact on BET surface area of modified carbon, which can be observed from Table 2. The BET surface area of modified carbon increases gradually from 941.78 to 956.46 m^2/g when the concentration of

sodium thiosulfate changes from 2 to 10 g/L; however, the BET surface area decreases sharply when the concentration of sodium thiosulfate continues to increase. It may be explained that a large amount of residual sodium thiosulfate are adsorbed onto the surface of activated carbon with the increasing concentration of sodium thiosulfate, and thus blocking the pores of activated carbons, leading to the decrease of BET surface area. Therefore, the concentration of sodium thiosulfate has significant impact on the BET surface area of activated carbon and 2 g/L was chosen as the optimum modification concentration, referring to as TDAC-ST.

The pore structures of activated carbons are presented in Fig. 2 and porous structure parameters of
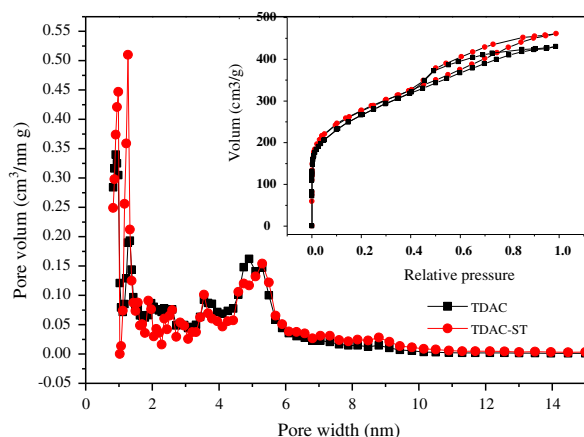
Fig. 2. Pore size distributions of TDAC and TDAC-ST and N$_2$ adsorption/desorption isotherms (inset).

both samples, including S_{BET}, V_{tot} and D_P, were calculated and summarized in Table 3. It can be seen that TDAC-ST displays the higher pore volume (0.69 cm^3/g) than TDAC (0.64 cm^3/g), indicating that the pore structure of activated carbon was better developed after modification. The distribution of pore size for the two adsorbents shows that the majority of pore size is smaller than 10 nm, suggesting that most of the pores are micropore and mesopore.

3.1.2. Surface chemical characteristics of TDAC and TDAC-ST

The surface functional group is an important characteristic of activated carbons since it has significant implications on their behaviors as catalysts, ion exchanges, adsorbents, and catalyst support and determines the surface properties of the carbons [24]. The FTIR spectra of TDAC and TDAC-ST before and after adsorption are presented in Fig. 3. TDAC and TDAC-ST have similar peaks at 3,361, 1,584, 1,171, 1,073, 495 cm^{-1}. The peak at 3,361 cm^{-1} is from O–H stretch for carboxyl and phenol functional groups or adsorbed water and the asymmetric peak

shape is characteristic of hydrogen bonding. The intense bands appearing around 1,580 cm^{-1} are the result of C=O stretches in aromatic ring. The bands between 1,000 and 1,200 cm^{-1} can be attributed to the C–C and C–O vibrations in acids, alcohols, phenols, ethers, and esters. The peak at 495 cm^{-1} is from C-Br, which is a result of KBr-C tablet. The peak intensity of TDAC-ST is stronger than that of TDAC, especially at 1,580, and 1,000–1,200 cm^{-1}, which reflects that sodium thiosulfate may interact with the TDAC surface groups.

3.1.3. Element analysis of TDAC and TDAC-ST

Element analysis was carried out to investigate the complete element analysis composition of TDAC and TDAC-ST as shown in Table 2, the major elements of adsorbents are carbon and oxygen, phosphorus comes from phosphoric acid, magnesium and calcium element may be the result of tap water used in the process of washing carbon. Sodium and sulfur element are detected in TDAC-ST compared with TDAC which indicates that sodium thiosulfate is adsorbed on the surface of the activated carbon.

3.2. The effect of contact time and adsorption kinetics of STM onto adsorbents

Information on the kinetics of STM removal is essential to determine the optimum operation time for batch experiments. The effects of contact time of STM onto TDAC and TDAC-ST are presented in Fig. 4. For both adsorbents, about 85% of the adsorption capacity was fulfilled within the third hour of contact. The adsorption speed was rapid initially and then decelerated. The adsorption equilibrium was gradually reached within 1,440 min. Moreover, Fig. 4 also shows that TDAC-ST has larger equilibrium uptake than TDAC. Such phenomenon indicated that although BET surface area of adsorbent acted as one of the significant factor that influenced the adsorption of STM, other significant factor that influenced the adsorption

Table 3
Porous structure parameters of TDAC and TDAC-ST

Type	S_{BET}[a] (m^2/g)	S_{mic}[b] (m^2/g)	(%)	S_{ext}[c] (m^2/g)	(%)	V_{tot}[d] (cm^3/g)	V_{mic}[e] (cm^3/g)	(%)	V_{ext}[f] (cm^3/g)	(%)	D_P[g] (nm)
TDAC	949.36	529.67	55.8	419.69	44.2	0.64	0.26	40.6	0.38	59.4	2.70
TDAC-ST	941.94	515.04	54.7	426.90	45.3	0.69	0.27	39.1	0.42	60.9	2.93

[a]BET surface area. [b]Micropore surface area. [c]External surface area. [d]Total pore volume. [e]Micropore volume. [f]External volume. [g]Mean pore diameter.
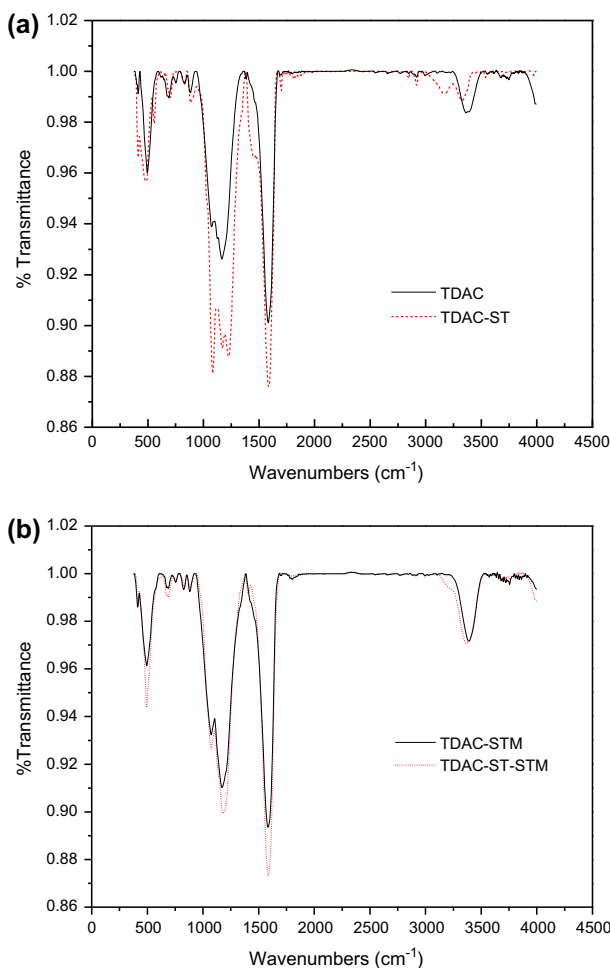
Fig. 3. FTIR spectra of TDAC and TDAC-ST before (a) and after (b) adsorption.
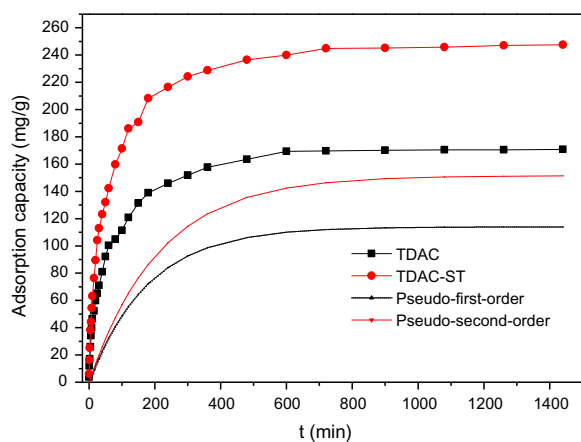

Fig. 4. Effect of contact time on adsorption of STM onto TDAC/TDAC-ST and adsorption kinetics.

capacity was the surface chemistry of the adsorbents. As mentioned previously, TDAC had slight larger surface area but lower acidic functional group than TDAC-ST, suggesting that acidic functional group had a positive influence on STM adsorption. In order to ensure sufficient contact time, further adsorption experiments were performed for 1,440 min.

The study of kinetics could help attain the possible mechanism of adsorption as well as the reaction pathways [25]. Former researches have divided the major interactions into pseudo-first-order and pseudo-second-order kinetics in light of the fitting degree. In order to understand the mechanism involved in the adsorption, two commonly used adsorption kinetic models, pseudo-first-order and pseudo-second-order were employed for the experimental data.

The linear form of the pseudo-first-order equation [26] can be expressed as:

$$\ln(q_e - q_t) = \ln q_e - k_1 t \tag{4}$$

where q_e and q_t (mg/g) are the amounts of STM adsorbed at equilibrium and at time t (min), respectively, and k_1 (1/min) is the rate constant of the pseudo-first-order model. The values of q_e and k_1 can be obtained from the intercept and slope of a plot of $\ln (q_e-q_t)$ vs. t.

The linear form of the pseudo-second-order equation [27] is given as follows:

$$\frac{t}{q_t} = \frac{1}{k_2 q_e^2} + \frac{1}{q_e} t \tag{5}$$

where k_2 (g/(mg min)) is the pseudo-second-order rate constant. The parameters q_e and k_2 can be estimated from the slope and the intercept of the plot (t/q_t) vs. t.

The comparison of the pseudo-first-order and pseudo second-order model for the adsorption of STM onto TDAC and TDAC-ST is illustrated in Fig. 5. The calculated kinetic parameters, correlation coefficients are listed in Table 4. Compared with pseudo-first-order kinetic, pseudo-second-order kinetic model was more appropriate to depict the kinetic data, which can be drawn by higher R^2 and the correspondence on $q_{e,exp}$ and $q_{e,cal}$. The result indicates that the rate-limiting step in the adsorption of STM are chemisorptions involving valence forces through sharing of exchanging electrons between adsorbent and adsorbate [28]. These observations were consistent with the electrostatic interaction or ion exchange adsorption mechanisms, proposed in the following discussion.
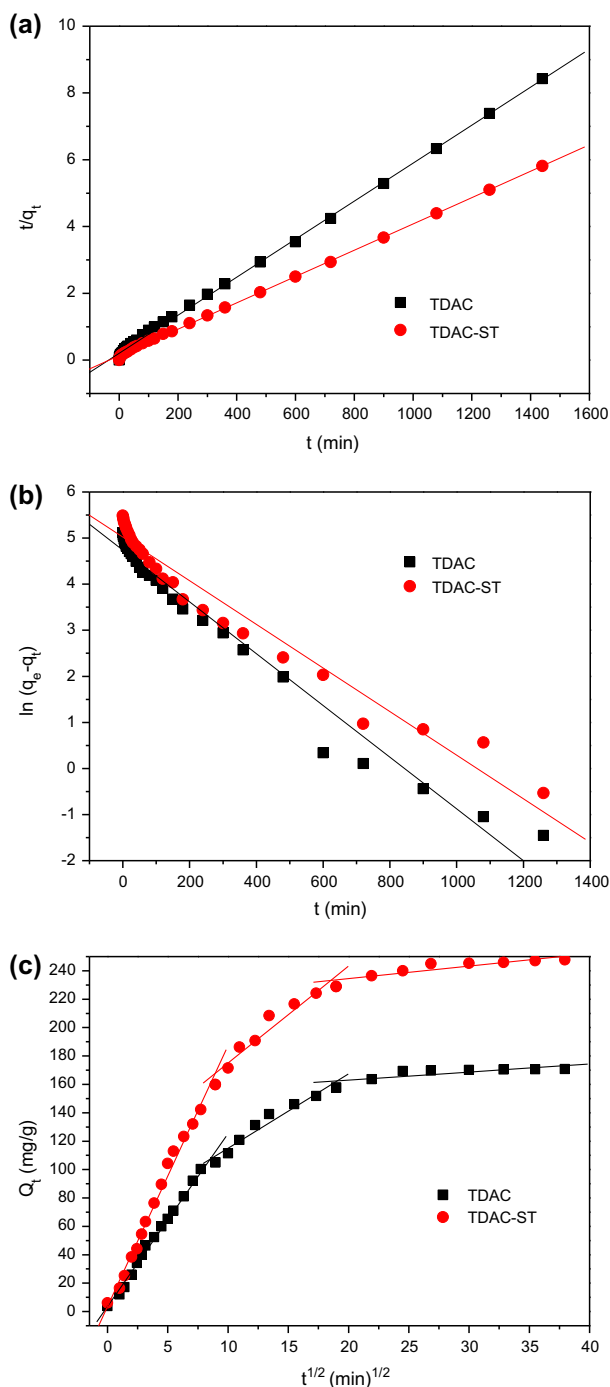
Fig. 5. Pseudo-first-order kinetics equation curve (a), pseudo-second-order kinetics equation curve (b), intraparticle diffusion equation, and (c) fit of the adsorption kinetics.

In order to further investigate the adsorption mechanism, the intraparticle diffusion model was also used to analyze the kinetic results. The intraparticle diffusion model [29] is expressed as follows:

$$q_t = k_{pi}t^{1/2} + C \qquad (6)$$

where q_t (mg/g) is the amount of STM adsorbed at time t (min), k_{pi} (mg/g min$^{1/2}$) is the intraparticle diffusion rate constant, and C (mg/g) represents the thickness of the boundary layer [30].

Fig. 4 shows that the intraparticle diffusion model plots presented multilinearity for both adsorbents, indicating that three steps occurred in the adsorption process. The first sharp stage was attributed to the diffusion of STM from the solution to the external surface of the adsorbent. The second stage was gradual adsorption, where intraparticle diffusion was rate limiting. For the last step, the diffusion slowed down and adsorption finally reached equilibrium, due to low concentration of STM and reduction of interior active sites [31]. It can be explained that abundant vacant surface active sites were available for adsorption at the initial stage, after that, the rest of vacant surface sites became difficult to occupy because of the low STM concentration left in solution, the decrease of interior active sites as well as the repulsive forces between the adsorbates and the bulk phase [32].

3.3. Adsorption isotherms for the adsorption of STM onto adsorbents

Adsorption isotherm is significant to investigate the adsorption capacity of adsorbents and understand the nature of the solute–surface interaction. Adsorption isotherms were analyzed at various temperatures (303, 313 and 323 K). Three commonly used models, Langmuir [31], Freundlich [33] and Temkin [34] isotherm models were employed for the experiment data.

The Langmuir model is based on the assumption that adsorption was complete homogeneous [35] and the Langmuir equation is presented as follows:

$$\frac{C_e}{Q_e} = \frac{1}{Q_0 K_L} + \frac{1}{Q_0}C_e \qquad (7)$$

where C_e (mg/L) represents the equilibrium STM concentration, Q_e (mg/g) is the amount of STM adsorbed at equilibrium, Q_0 (mg/g) is the maximum adsorption capacity, and K_L (L/mg) is the Langmuir constant.

Freundlich isotherm model assumes that heterogeneous adsorbent surface with several adsorption energies at different sites [36]. The Freundlich isotherm equation is expressed as follows:

Table 4
Kinetics parameters of the STM adsorption onto TDAC/TDAC-ST

Samples	$q_{e,exp}$ (mg/g)	Pseudo-first-order parameters				Pseudo-second-order parameters		
		$K_1 \times 10^{-3}$ (mg/g min)	$q_{e,cal}$ (mg/g)	R^2		$K_2 \times 10^{-4}$ (mg/g min)	$q_{e,cal}$ (mg/g)	R^2
TDAC	170.8372	5.6	114.0686	0.9718		1.57	175.4386	0.9989
TDAC-ST	247.6522	4.7	151.5931	0.9594		1.13	256.4103	0.9993

$$\ln Q_e = \ln K_F + \frac{1}{n} \ln C_e \qquad (8)$$

where Q_e (mg/g) is the amount of STM adsorbed at equilibrium, C_e (mg/L) is the equilibrium concentration of STM, K_F (mg/g (L/mg)$^{1/n}$) is the empirical constant of adsorption capacity, and n presents the favorable degree of the adsorption process. The adsorption is unfavorable adsorption ($n < 1$) [37] or preferential adsorption ($n > 1$).

Temkin model is on the basis of uniform distribution of binding energies [34]. The equation is as follows:

$$Q_e = A \ln K_T + A \ln C_e \qquad (9)$$

where $A = RT/b$, T (K) is the absolute temperature (K), R is the gas constant (8.314 J/(mol K)). K_T (L/mg) is the Temkin isotherm constant.

The fitting results calculated from three isotherms are given in Table 5. The results indicated that the adsorption of STM onto both adsorbents was temperature-dependent. The adsorbed amounts of STM increased with increasing temperature. It seemed that the higher temperature provided the potential activation energy that was required to change reactants into activated complex, resulting in the increase of the adsorption capacity for the activated adsorption.

Table 5
Isotherm model constants for STM adsorption onto TDAC-ST

Isotherms	Parameters	Temperature (K)		
		303	313	323
Langmuir	Q_m (mg/g)	256.41	263.16	270.27
	K_1 (L/mg)	0.0445	0.0668	0.0814
	R^2	0.9996	0.9985	0.9993
Freundlich	K_F ((mg/g)(L/mg)$^{1/n}$)	50.41	58.13	61.64
	n	2.88	3.29	4.86
	R^2	0.9152	0.9491	0.9329
Temkin	K_T (L/mg)	121.93	124.92	126.84
	A	39.17	37.74	35.23
	R^2	0.9503	0.9205	0.9671

Furthermore, higher temperature seemed to have a swelling effect in the internal structure of the adsorbents and thus enabling large STM molecules to penetrate further. Moreover, it could also be observed from Table 5 that the values of linear correlation coefficient of three models were all higher than 0.91, while for Langmuir isotherm were between 0.9985 and 0.9996 relatively larger values of R^2 than that of the other isotherms, which means that Langmuir isotherm fit the equilibrium data very well. It suggests that activated sites are homogeneously distributed on the TDAC-ST surface and a monolayer of STM covers on TDAC-ST surface. The values of n are larger than one for all temperatures, which demonstrates that STM adsorption onto TDAC-ST is favorable [32]. The values of Q_m and K_L increased with temperature, indicating the adsorption process was endothermic.

3.4. Effect of initial STM concentration

The effect of initial concentration on STM removal by TDAC and TDAC-ST was investigated by performing the experiments at various initial concentrations of STM (25–400 mg/L) with 0.1 g of adsorbent. As illustrated in Fig. 6, the adsorption capacities increase sharply as the concentration of STM increases from 25
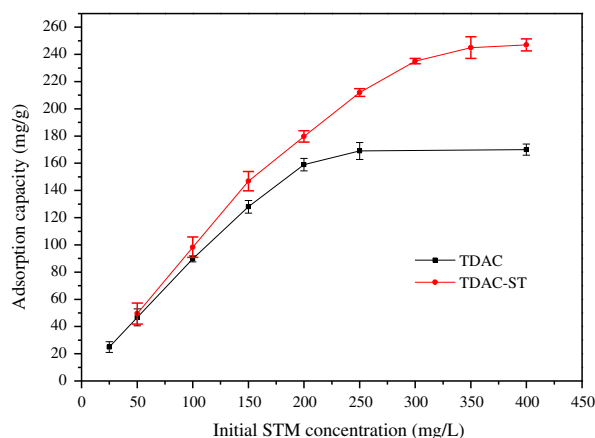

Fig. 6. Effect of initial concentration on adsorption of STM on TDAC and TDAC-ST.

to 200 mg/L. Then, the adsorbed amount of STM for TDAC remains a constant value of 170 mg/g, while TDAC-ST continues to increase and finally the adsorption capacity reaches 245 mg/g at the maximum STM concentration of 400 mg/L.

TDAC-ST exhibits a much stronger adsorption capacity for STM compared with TDAC, which is about 1.5 times of the latter. Impregnation with sodium thiosulfate could greatly improve the adsorption capacity of TDAC for STM removal. This improvement may be explained that sodium thiosulfate was loaded on TDAC-ST surface and reacted with STM as a reducing agent.

3.5. Effect of solution pH

Solution pH has proved to be a significant influential factor that affects the adsorption on activated carbon [38], as it can alter the surface charge of STM and the adsorbent surface properties. The effect of pH on STM adsorption on TDAC and TDAC-ST is illustrated in Fig. 7. Initial STM solution pH is around 6. It can be seen that adsorption of STM onto TDAC and TDAC-ST is pH-dependent. Adsorption capacity increases with increasing pH in the entire pH range studied (between 2 and 11), especially for TDAC-ST. STM removal ranges from 125 to 167 mg/g for TDAC as pH increases from 2 to 11. But for TDAC-ST, the corresponding value is from 180 to 315 mg/g, which exhibits higher adsorption capacity than the former.

In the pH range between 2 and 7, the weak adsorption capability may be attributed to the electrostatic repulsive force between STM and the adsorbent surface. The electrostatic repulsive force was growing insensitively at lower pH and thus resulting in the
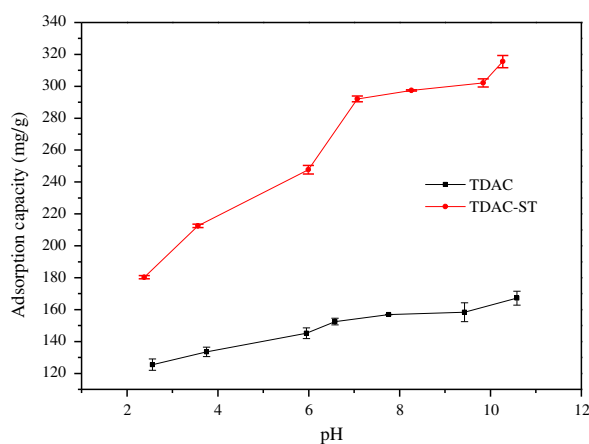
Table 6
Thermodynamic parameters for STM adsorption on TDAC-ST calculated under standard conditions

Samples	T (K)	ΔG^0 (kJ/mol)	ΔH^0 (kJ/mol)	ΔS^0 (J/mol K)
TDAC	303	−26.89	28.96	143.69
	313	−28.45		
	323	−29.98		
TDAC-ST	303	−25.60	24.65	166.26
	313	−27.50		
	323	−28.91		

decrease of adsorption capacity of both adsorbents with increasing acidity of the solution. In addition, such phenomenon may be related to the character of STM at lower pH, STM reacts with H^+ to form the positively charged ionic compounds that will affect STM properties and thus decreasing STM adsorption onto activated carbon. Moreover, when the pH varies from 7 to 11, the STM uptake increased with increasing pH may be attributed to the result that STM turned to be nonpolar and basic groups of activated carbon increased. In addition, no effort was made to maintain pH of the solution constant, and it was found that pH of the solution decreased with adsorption and TDAC-ST caused larger decrease. Liu et al. [39] proposed that the exchange of released H^+ occurred between the adsorbent surface and solution resulting in decreasing of pH, indicating that the removal of STM from solution onto the adsorbents was partly related to cation-exchange mechanism.

3.6. Thermodynamics

Adsorption thermodynamics provide important information about thermodynamic performances of STM adsorption onto TDAC-ST. The enthalpy change (ΔH^0), Gibbs free energy change (ΔG^0), and entropy change (ΔS^0) can be calculated according to the Gibbs free energy equations [40,41]:

$$\Delta G^0 = -RT \ln K \tag{10}$$

$$\ln K = \frac{\Delta S^0}{R} - \frac{\Delta H^0}{RT} \tag{11}$$

where R is the gas law constant (8.314 J/(mol K)), T (K) is the absolute temperature and K (L/mol) is the Langmuir constant corresponding to determined temperature. The values of ΔH^0 and ΔS^0 can be calculated from the slope and intercept of the Van't Hoff plot of $\ln K$ vs. $(1/T)$.

Fig. 7. Effect of solution pH on adsorption of STM on TDAC and TDAC-ST.

Based on the results in Table 6, the negative values ΔG^0 suggested that the adsorption of STM onto adsorbents was spontaneous and thermodynamically favorable [42]. The value of ΔH^0 indicated that the endothermic nature of the adsorption of STM onto TDAC-ST, which is confirmed by the increasing adsorption of STM with the increase in temperature. Moreover, the positive ΔS^0 revealed the affinity of STM onto adsorbent and increased randomness at the solid/solution interface during the adsorption.

4. Conclusions

In this study, a novel approach was proposed to prepare modified activated carbon and removal of STM from aqueous solutions was investigated. The results indicated that sodium thiosulfate–modified activated carbon prepared from *T. dealbata* proved to be an effective adsorbent to remove STM from aqueous solutions. TDAC-ST had slightly smaller BET surface area but more acidic functional groups and preferable adsorption capacity as compared to TDAC. The adsorption of STM by both adsorbents was most favorable under alkaline conditions, especially for TDAC-ST. The adsorption kinetics of both adsorbents was in good agreement with the pseudo-second-order model. Experimental equilibrium data followed the Langmuir models and the maximum adsorption capacity for TDAC-ST was 256.41 mg/g as calculated by Langmuir equation. Adsorption thermodynamics indicated that the adsorption of STM onto TDAC-ST was spontaneous, favorable and endothermic.

Acknowledgements

References

[1] H.M. Ötker, I. Akmehmet-Balcıoğlu, Adsorption and degradation of enrofloxacin, a veterinary antibiotic on natural zeolite, J. Hazard. Mater. 122 (2005) 251–258.

[2] S.H. Kim, H.K. Shon, H.H. Ngo, Adsorption characteristics of antibiotics trimethoprim on powdered and granular activated carbon, J. Ind. Eng. Chem. 16 (2010) 344–349.

[3] M. Teuber, Veterinary use and antibiotic resistance, Curr. Opin. Microbiol. 4 (2001) 493–499.

[4] A.G. Trovó, R.F. Pupo Nogueira, A. Agüera, A.R. Fernandez-Alba, S. Malato, Degradation of the antibiotic amoxicillin by photo-Fenton process—Chemical and toxicological assessment, Water Res. 45 (2011) 1394–1402.

[5] T.-H. Yu, A.Y.-C. Lin, S.C. Panchangam, P.-K.A. Hong, P.-Y. Yang, C.-F. Lin, Biodegradation and bio-sorption of antibiotics and non-steroidal anti-inflammatory drugs using immobilized cell process, Chemosphere 84 (2011) 1216–1222.

[6] R. Tompsett, W. McDermott, Recent advances in streptomycin therapy, Am. J. Med. 7 (1949) 371–381.

[7] J. Xie, A.E. Talaska, J. Schacht, New developments in aminoglycoside therapy and ototoxicity, Hearing Res. 281 (2011) 28–37.

[8] T.D. Brock, R.M. Johnson, W.B. DeVille, Physical and chemical properties of a bacterial virus as related to its inhibition by streptomycin, Virology 25 (1965) 439–453.

[9] F.R. Balyan, A. Taibah, G.D. Donato, A. Aslan, M. Falcioni, A. Russo, M. Sanna, Titration streptomycin therapy in Meniere's disease: Long-term results, Otolaryngol. Head Neck 118 (1998) 261–266.

[10] T.-H. Yu, A.Y.-C. Lin, S.K. Lateef, C.-F. Lin, P.-Y. Yang, Removal of antibiotics and non-steroidal anti-inflammatory drugs by extended sludge age biological process, Chemosphere 77 (2009) 175–181.

[11] W. Ben, Z. Qiang, X. Pan, M. Chen, Removal of veterinary antibiotics from sequencing batch reactor (SBR) pretreated swine wastewater by Fenton's reagent, Water Res. 43 (2009) 4392–4402.

[12] K.-J. Choi, S.-G. Kim, S.-H. Kim, Removal of antibiotics by coagulation and granular activated carbon filtration, J. Hazard. Mater. 151 (2008) 38–43.

[13] A. Dąbrowski, P. Podkościelny, Z. Hubicki, M. Barczak, Adsorption of phenolic compounds by activated carbon—A critical review, Chemosphere 58 (2005) 1049–1070.

[14] L. Huang, Y. Sun, W. Wang, Q. Yue, T. Yang, Comparative study on characterization of activated carbons prepared by microwave and conventional heating methods and application in removal of oxytetracycline (OTC), Chem. Eng. J. 171 (2011) 1446–1453.

[15] C. Namasivayam, D. Kavitha, Removal of Congo Red from water by adsorption onto activated carbon prepared from coir pith, an agricultural solid waste, Dyes Pigm. 54 (2002) 47–58.

[16] C.Y. Yin, M.K. Aroua, W.M.A.W. Daud, Review of modifications of activated carbon for enhancing contaminant uptakes from aqueous solutions, Sep. Purif. Technol. 52 (2007) 403–415.

[17] W. Liu, J. Zhang, C. Zhang, Y. Wang, Y. Li, Adsorptive removal of Cr (VI) by Fe-modified activated carbon prepared from Trapa natans husk, Chem. Eng. J. 162 (2010) 677–684.

[18] H. Liu, W. Liu, J. Zhang, C. Zhang, L. Ren, Y. Li, Removal of cephalexin from aqueous solutions by original and Cu(II)/Fe(III) impregnated activated carbons developed from lotus stalks kinetics and equilibrium studies, J. Hazard. Mater. 185 (2011) 1528–1535.

[19] J. Zhang, Q. Shi, C. Zhang, J. Xu, B. Zhai, B. Zhang, Adsorption of Neutral Red onto Mn-impregnated activated carbons prepared from Typha orientalis, Bioresour. Technol. 99 (2008) 8974–8980.

[20] G. Schlieper, V. Brandenburg, M. Ketteler, J. Floege, Sodium thiosulfate in the treatment of calcific uremic arteriolopathy, Nat. Rev. Nephrol. 5 (2009) 539–543.

[21] C.G. Le Prell, D. Yamashita, S.B. Minami, T. Yamasoba, J.M. Miller, Mechanisms of noise-induced hear-

ing loss indicate multiple methods of prevention, Hearing Res. 226 (2007) 22–43.

[22] T.-T. Zhang, L.-L. Wang, Z.-X. He, D.Zhang, Growth inhibition and biochemical changes of cyanobacteria induced by emergent macrophyte Thalia dealbata roots, Biochem. Syst. Ecol. 39 (2011) 88–94.

[23] B. Morelli, Simultaneous determination of ceftriaxone and streptomycin in mixture by 'ratio-spectra' 2nd derivative and 'zero-crossing' 3rd derivative spectro-photometry, Talanta 41 (1994) 673–683.

[24] T. Budinova, E. Ekinci, F. Yardim, A. Grimm, E. Björnbom, V. Minkova, M. Goranova, Characterization and application of activated carbon produced by H_3PO_4 and water vapor activation, Fuel Process. Technol. 87 (2006) 899–905.

[25] S. Sen Gupta, K.G. Bhattacharyya, Kinetics of adsorption of metal ions on inorganic materials: A review, Adv. Colloid Interface Sci. 162 (2011) 39–58.

[26] J. Zhang, Y. Li, C. Zhang, Y. Jing, Adsorption of malachite green from aqueous solution onto carbon prepared from Arundo donax root, J. Hazard. Mater. 150 (2008) 774–782.

[27] Y.S. Ho, G. McKay, Pseudo-second order model for sorption processes, Process Biochem. 34 (1999) 451–465.

[28] J. Febrianto, A.N. Kosasih, J. Sunarso, Y.-H. Ju, N. Indraswati, S. Ismadji, Equilibrium and kinetic studies in adsorption of heavy metals using biosorbent: A summary of recent studies, J. Hazard. Mater. 162 (2009) 616–645.

[29] D. Kavitha, C. Namasivayam, Experimental and kinetic studies on methylene blue adsorption by coir pith carbon, Bioresour. Technol. 98 (2007) 14–21.

[30] A. El Nemr, A. Khaled, O. Abdelwahab, A. El-Sikaily, Treatment of wastewater containing toxic chromium using new activated carbon developed from date palm seed, J. Hazard. Mater. 152 (2008) 263–275.

[31] F.-C. Wu, R.-L. Tseng, R.-S. Juang, Comparisons of porous and adsorption properties of carbons activated by steam and KOH, J. Colloid Interface Sci. 283 (2005) 49–56.

[32] Y. Yao, F. Xu, M. Chen, Z. Xu, Z. Zhu, Adsorption behavior of methylene blue on carbon nanotubes, Bioresour. Technol. 101 (2010) 3040–3046.

[33] E.N. El Qada, S.J. Allen, G.M. Walker, Adsorption of Methylene Blue onto activated carbon produced from steam activated bituminous coal: A study of equilibrium adsorption isotherm, Chem. Eng. J. 124 (2006) 103–110.

[34] K.Y. Foo, B.H. Hameed, Insights into the modeling of adsorption isotherm systems, Chem. Eng. J. 156 (2010) 2–10.

[35] K.T. Ranjit, I. Willner, S.H. Bossmann, A.M. Braun, Lanthanide oxide doped titanium dioxide photocatalysts: Effective photocatalysts for the enhanced degradation of salicylic acid and t-cinnamic acid, J. Catal. 204 (2001) 305–313.

[36] K. Vijayaraghavan, T.V.N. Padmesh, K. Palanivelu, M. Velan, Biosorption of nickel(II) ions onto sargassum wightii: Application of two-parameter and three-parameter isotherm models, J. Hazard. Mater. 133 (2006) 304–308.

[37] F. Haghseresht, G.Q. Lu, Adsorption characteristics of phenolic compounds onto coal-reject-derived adsorbents, Energy Fuels 12 (1998) 1100–1107.

[38] H. Demiral, G. Gündüzoğlu, Removal of nitrate from aqueous solutions by activated carbon prepared from sugar beet bagasse, Bioresour. Technol. 101 (2010) 1675–1680.

[39] W. Liu, J. Zhang, C. Zhang, L. Ren, Preparation and evaluation of activated carbon-based iron-containing adsorbents for enhanced Cr(VI) removal: Mechanism study, Chem. Eng. J. 189–190 (2012) 295–302.

[40] D. Mohan, V.K. Gupta, S.K. Srivastava, S. Chander, Kinetics of mercury adsorption from wastewater using activated carbon derived from fertilizer waste, Colloids Surf. 177 (2000) 169–181.

[41] G. McKay, M.J. Bino, A.R. Altamemi, The adsorption of various pollutants from aqueous solutions on to activated carbon, Water Res. 19 (1985) 491–495.

[42] Y. Wang, B.-Y. Gao, W.-W. Yue, Q.-Y. Yue, Preparation and utilization of wheat straw anionic sorbent for the removal of nitrate from aqueous solution, J. Environ. Sci. 19 (2007) 1305–1310.